

Scaling rules for the final decline to extinction

Blaine D. Griffen* and John M. Drake

Odum School of Ecology, University of Georgia, Athens, GA 30605, USA

Space–time scaling rules are ubiquitous in ecological phenomena. Current theory postulates three scaling rules that describe the duration of a population’s final decline to extinction, although these predictions have not previously been empirically confirmed. We examine these scaling rules across a broader set of conditions, including a wide range of density-dependent patterns in the underlying population dynamics. We then report on tests of these predictions from experiments using the cladoceran *Daphnia magna* as a model. Our results support two predictions that: (i) the duration of population persistence is much greater than the duration of the final decline to extinction and (ii) the duration of the final decline to extinction increases with the logarithm of the population’s estimated carrying capacity. However, our results do not support a third prediction that the duration of the final decline scales inversely with population growth rate. These findings not only support the current standard theory of population extinction but also introduce new empirical anomalies awaiting a theoretical explanation.

Keywords: carrying capacity; *Daphnia magna*; population extinction; population growth rate; scaling rule

1. INTRODUCTION

The consistency of certain spatial and temporal dynamics among highly different nonlinear ecological systems is astounding (Damuth 1998; Schneider 2001). Such scaling rules have been found to characterize individual behaviour (e.g. Sims *et al.* 2008); the use of space by organisms (Jetz *et al.* 2004); life-history patterns of individuals (e.g. Enquist *et al.* 1999); population growth, regulation and abundance (e.g. Belgrano *et al.* 2002); community stability (Otto *et al.* 2007); and, by integrating across species ensembles, even patterns of biodiversity across regional landscapes (e.g. Bellwood & Hughes 2001; Volkov *et al.* 2007). Focusing at the population level, recent work has highlighted scaling rules for population dynamics, including the scaling rules for demographic stochasticity (Desharnais *et al.* 2006), population size (Carbone & Gittleman 2002) and population growth rate (Savage *et al.* 2004).

Scaling rules for population persistence time also have been empirically examined (e.g. Diamond 1984; Belovsky *et al.* 1999). These studies confirm that population extinction risk is negatively correlated with habitat area, population density, carrying capacity and individual longevity, and is positively correlated with the variation in population size and environmental variability. However, a population’s persistence time (i.e. the total time it exists before extinction) may be independent of the speed with which it disappears once it has started its final decline to extinction. Understanding this final decline to extinction could provide useful information for conservation by informing the amount of time available for implementing conservation strategies to avoid extinction.

Recently, Lande *et al.* (2003) have proposed scaling rules for the duration of the final decline of a population to extinction. They derived these scaling rules using a model based on a diffusion process confined to the interval between extinction and a fixed ceiling. Models of this sort are commonly used to represent population growth in a randomly fluctuating environment (e.g. Lande *et al.* 2006) and are standard in conservation biology (e.g. Lande 1993; Middleton *et al.* 1995; Meir & Fagan 2000; Morris & Doak 2002). The new approach taken by Lande *et al.* (2003) was to introduce an interval between some small positive population size (extinction or quasi-extinction) and larger population size (carrying capacity) and study the *conditional* diffusion process that enters the interval from above and proceeds to cross the (quasi-)extinction boundary without returning to the upper boundary. Such a process can be interpreted as the process of a population’s final decline. From their analysis (Lande *et al.* 2003, pp. 47–49), we have the following hypotheses (figure 1).

Hypothesis 1.1. If a population starts at carrying capacity (K), and if it has a positive long-run growth rate when it is below K , then the expected duration of the final decline, T_E , from K to extinction (or to quasi-extinction, T_Q) is generally much shorter than the mean persistence time of the population before extinction, T_K , i.e. $T_E \ll T_K$.

Hypothesis 1.2. The duration of the final approach to extinction, T_E (or T_Q), increases logarithmically with increasing carrying capacity, i.e. $T_E \propto \ln(K)$.

Hypothesis 1.3. The duration of the final approach to extinction, T_E (or T_Q), is inversely proportional to the intrinsic growth rate, i.e. $T_E \propto 1/\ln(\lambda)$.

Importantly, these scaling rules were derived using a ceiling model, in which population growth is assumed to be density independent up to some reflecting boundary or carrying capacity, K , after which growth is density dependent. Since such processes are not typical

* Author and address for correspondence: Department of Biological Sciences and Marine Science Program, University of South Carolina, Columbia, SC 29208, USA (bgriffen@biol.sc.edu).

Electronic supplementary material is available at <http://dx.doi.org/10.1098/rspb.2008.1558> or via <http://journals.royalsociety.org>.

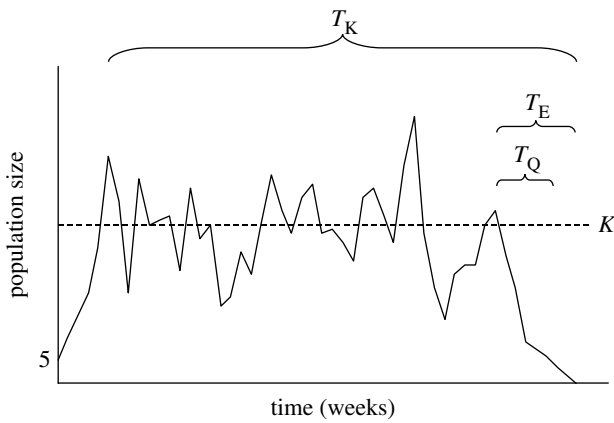


Figure 1. Illustration defining the variables T_K , T_E and T_Q .

(Sibly *et al.* 2005), our first goal was to establish the generality of these rules within a larger class of models of which the ceiling model studied by Lande *et al.* (2003) is a special case. Second, we sought empirical support for these putative scaling rules using data on extinction trajectories in laboratory populations of *Daphnia magna* (Griffen & Drake 2008a). Support for hypothesis 1.2 is available for vertebrate populations (Fagan & Holmes 2006), but to our knowledge hypotheses 1.1 and 1.3 have not been examined. We show that the scaling rule given in hypothesis 1.1 is indeed predicted for populations characterized by a large class of density-dependent population growth processes, and that this hypothesis is supported by extinction trajectories of empirical populations. However, we show that the scaling rules given in hypotheses 1.2 and 1.3 are only predicted for populations where growth is approximately density independent up to K , and further that these scaling rules are only partially supported by empirical data. These findings represent an important step towards predicting population extinction dynamics.

2. MATERIAL AND METHODS

(a) Extension of theoretical scaling rules

Lande *et al.* (2003) derived the scaling rules given in hypotheses 1.1–1.3 using a ceiling model with demographic and environmental stochasticity. To study these scaling rules in more generality, we require a model that takes as some limiting form the logistic ceiling model of Lande *et al.* (2003), but has the flexibility to represent a broader range of forms of density dependence. The model must also incorporate environmental and demographic stochasticity, and, for comparison, should be amenable to analysis as a diffusion process as in Lande *et al.* (2003). To develop such a model, we start with a recursion equation of the form

$$N_{t+1} \sim f(N_t), \quad (2.1)$$

in which the left-hand side, a random number representing population size, is distributed according to probability mass function f that depends on population size N at time t .

We chose model equations and parameters so that the expectation of N_{t+1} is the well-known theta-Ricker equation, a commonly used discrete analogue of the continuous time logistic model (Turchin 2003)

$$E[N_{t+1}] = N_t \exp\left(\lambda \left(1 - \left(\frac{N_t}{K}\right)^\theta\right)\right), \quad (2.2)$$

where λ is the maximum population growth rate; K is the carrying capacity; and θ is the scaling parameter that determines the importance of density dependence. Then, with $\theta = \infty$, we recapture the logistic ceiling conditions of Lande *et al.* (2003), while for $0 < \theta < \infty$ we represent a wide spectrum of possibilities for the form of density dependence.

We incorporated environmental and demographic stochasticity as follows. The term in the right-hand side of equation (2.2) contained within the outer brackets can be viewed as a density-dependent growth rate, which we denote by λ_N . We incorporated environmental stochasticity by considering λ_N to be a random variable, unique for each t . As a growth rate, it must be positive and continuously distributed. The gamma distribution is a flexible distribution with these properties, and we therefore assumed that λ_N was drawn from a gamma distribution. We incorporated demographic stochasticity by assuming that the population size at time t was a discrete random variable with a mean equal to λ_N . We assumed that reproductive events were independent and could therefore be represented by a Poisson distribution with rate parameter equal to the gamma-distributed random variable, λ_N . Probability distributions in which the parameters themselves are random variables are known as mixture distributions. The parametrized version of equation (2.2) thus included environmental and demographic stochasticity using a gamma-mixed Poisson distribution (Johnson *et al.* 1993, p. 308), and can be approximated by a diffusion process with a mean

$$M(N) = E[N_{t+1}] - N_t = N_t \left(\exp\left(\lambda \left(1 - \left(\frac{N_t}{K}\right)^\theta\right)\right) - 1 \right), \quad (2.3)$$

and variance

$$V(N) = \frac{\exp\left(\lambda \left(1 - \left(\frac{N_t}{K}\right)^\theta\right)\right)}{(N_t \beta + 1)^{-1}}, \quad (2.4)$$

where β is the scale parameter of the gamma distribution which governs the degree of environmental stochasticity (see appendix I for a more complete description and a derivation of this model).

Our model simulations therefore followed Lande *et al.* (2003) by updating population size at $t+1$ as

$$N_{t+1} = N_t + M(N)dt + \left(\sqrt{V(N)dt}\right)B, \quad (2.5)$$

where dt is the increment of time used in the diffusion process (0.1), and B is a normally distributed random number representing Brownian motion occurring in the time increment dt . We extended the predictions of Lande *et al.* to a more general case by examining this model at $\theta = \{0.1, 0.25, 0.5, 1, 2, 4, 8, 16, 32, 64\}$.

We varied population growth rate $\lambda = \{1, 1.5, 2.0, 2.5, 3.0, 3.5, 4.0\}$ and carrying capacity $K = \{4, 8, 16, 32, 64, 128\}$ in our model simulations for each θ given above. Model simulations were started with $N_0 = K$ and continued until the population went extinct ($N_t \leq 0$, population sizes < 0 were possible with our discrete-time diffusion approximation). Simulations were replicated 100 times at each of the 420 combination of K , λ and θ described above. We also replicated this set of simulations over a range of values for $\beta = \{0.5, 2, 3.5, 5\}$ to determine whether these scaling rules changed depending on the strength of environmental stochasticity.

We determined the duration of the final decline to extinction, T_E , for each simulation by calculating the interval from the last time the population dipped below K until extinction (figure 1). The distributions of T_E and T_K from our simulated populations were both strongly right-skewed. We therefore determined whether the scaling rule given in hypothesis 1.1 above, $T_E \ll T_K$, held for model populations over the full range of values for θ by comparing T_E and T_K using a paired Wilcoxon signed-rank test at each θ . Next, we determined whether the scaling rule given in hypotheses 1.2 and 1.3 above, $T_E \propto \ln(K)$ and $T_E \propto 1/\ln(\lambda)$, held over the full range of values for θ using model comparison to select the best model from a field of alternatives comprising both the predicted scaling rules and the untransformed K and $\ln(\lambda)$ in all combinations. Thus, the following four linear models were fit to the simulated data, assuming a normal error distribution

- (1) $T_E = a(\ln(\lambda)) + bK + c$
- (2) $T_E = a\left(\frac{1}{\ln(\lambda)}\right) + bK + c$
- (3) $T_E = a(\ln(\lambda)) + b(\ln(K)) + c$
- (4) $T_E = a\left(\frac{1}{\ln(\lambda)}\right) + b(\ln(K)) + c$

where a and b are coefficients and c is the intercept. We then used AIC to determine which model provided the best fit to the simulated data. Model 4 is the model that agrees with both hypotheses 1.2 and 1.3, thus, selection of this model would concurrently support both of these hypotheses.

(b) Experiment

We tested for the presence of scaling rules in data from a two-factor, fully crossed experiment in which 96 laboratory populations of the ubiquitous herbivorous zooplankton *D. magna* were tracked until extinct. Experimental treatments were habitat size (small: 700 ml, large: 1400 ml) and amount of food provided (200, 400 or 800 $\mu\text{l d}^{-1}$). The food resource was a solution of processed *Spirulina* sp. (JEHM Co., Inc.), prepared by mixing 0.05 g *Spirulina* (a blue-green alga, 10.16% N, 44.96% C) into 25 ml of deionized water. Each treatment was replicated 16 times. Populations were started with one non-gravid adult and four juveniles on February 28, 2007 or March 1, 2007. Populations were censused weekly by counting all individuals. The experiment was complete when all populations were extinct (49 weeks).

Experimental chambers (31.5 × 21.7 × 1 or 2 cm—thickness depended on habitat size treatment) were made of clear Plexiglas and filled with synthetic freshwater medium (USEPA 2002). We exchanged 50 per cent of the medium monthly to prohibit build-up of metabolic by-products. Microcosms were located on a laboratory bench top, randomly ordered, in a room with 24 h fluorescent light and the temperature held constant at 23.3 ± 1.4°C (mean ± s.d.). For a detailed description of the experiment, see Griffen & Drake (2008a).

Three pieces of evidence demonstrate that our experimental populations were well characterized by a diffusion process, and thus provided a good test of the scaling rules given by Lande *et al.* (2003). First, populations generally changed in size by small increments. Second, there was a general increase in variance through time (as evidenced by a significant positive slope in the regression of $\text{abs}(N_{t+1} - N_t)$ against time, $p = 0.002$). Third, visual inspection of a frequency histogram of times to population extinction indicated that these times had a negative exponential distribution, as is expected with a diffusion process (Lande *et al.* 2003).

(c) Statistical examination of scaling rules

Two important parameters in the hypotheses given by Lande *et al.* (2003) are the intrinsic rate of increase, $\ln(\lambda)$, and the carrying capacity, K . We estimated both of these parameters simultaneously by fitting the Ricker model to each time series of population sizes from the experimental populations (all parameter estimates were significant at the 0.05 level). We then determined T_E and T_K for each experimental population as described above for the model-generated population data. We also performed a duplicate set of analyses with parameters that we estimated independently. Specifically, we estimated $\ln(\lambda)$ as $\hat{\lambda} = \ln(N_2/N_0)$, using N_2 rather than N_1 because the generation time in our experimental systems was approximately twice the length of our sampling interval (B. D. Griffen 2007, unpublished data), and using the median population size as an estimate of K . However, results with these parameter estimates were not qualitatively different from that when both parameters were estimated simultaneously using the Ricker model. We therefore report only the results with simultaneously estimated parameters.

While the experiment included a total of 96 populations (see Griffen & Drake 2008a), not all of these were included in the analyses. Hypotheses 1.1–1.3 above apply only to populations with positive long-run growth rates at population sizes below K (Lande *et al.* 2003). Fifty-one of the ninety-six experimental populations had $\hat{\lambda} \leq 1$. These populations were excluded from the analyses, leaving a total of 45 populations. There was a single outlying population that had T_E that was nearly twice that of any other population. However, the results of analyses were qualitatively the same with and without including this population. We therefore report only the results with this population included.

Hypotheses 1.1–1.3 apply equally to the decline to complete extinction and the decline to some previously stipulated population size, i.e. quasi-extinction (see figure 1). We tested each of these hypotheses using our experimental data for both the decline to complete extinction (population size = 0) and the decline to quasi-extinction (population size = 5). This provided two separate tests of each theory. T_E and T_Q were determined for each population using the same method as described above for the analysis of model-simulated populations.

Hypothesis 1.1 ($T_E \ll T_K$ and $T_Q \ll T_K$): As with model-simulated populations, the distributions of T_E , T_Q and T_K from our experimental populations were all strongly right-skewed. We therefore used a Wilcoxon signed-rank test to test the hypotheses that the duration of the final decline to extinction (T_E) or the decline to quasi-extinction (T_Q) are much shorter than the persistence time of the population after it first reaches \hat{K} and before extinction (T_K).

Hypotheses 1.2 and 1.3 (T_E and T_Q increase proportionally with $\ln(K)$ and with the inverse of $\ln(\lambda)$): The estimates of carrying capacity and the intrinsic rate of increase were positively correlated across populations (Pearson's correlation = 0.71, $p \ll 0.0001$). We therefore simultaneously tested the hypotheses that the duration of the final decline to extinction increases logarithmically with \hat{K} and with the inverse of $\ln(\hat{\lambda})$, using identical analyses as we used with model data.

Specifically, we tested hypotheses 1.2 and 1.3 by fitting the four linear models described above. As with the analysis of model data, we then used AIC to determine which of the four models best fit the experimental data. Model 4 is the model that agrees with both hypotheses 1.2 and 1.3, thus selection of

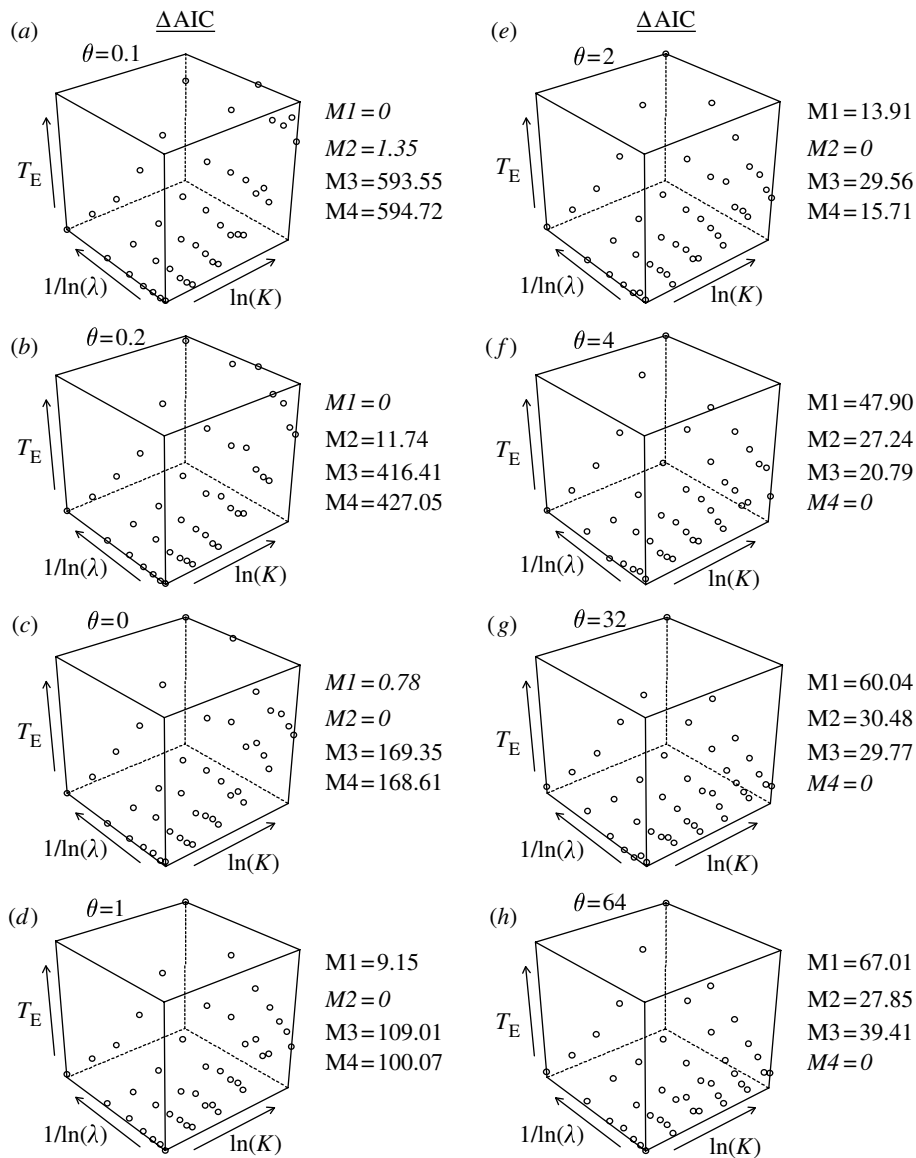


Figure 2. Scaling rules for the duration of the final decline to extinction (T_E) with $\ln(K)$ and $1/\ln(\lambda)$ over a range of density-dependent relationships based on theta-logistic model simulations. Data points indicate the mean of 100 replicate simulations at each combination of $\ln(K)$ and $1/\ln(\lambda)$. Italic ΔAIC values highlight models that provided the best fit to the simulated data at each θ .

this model would concurrently support both of these hypotheses. Some populations included in the analyses had values of $\hat{\lambda}$ which were only slightly greater than one, resulting in $\ln(\hat{\lambda})$ values that were very close to zero and $1/\ln(\hat{\lambda})$ values that were extremely large (i.e. outliers). To avoid this, we instead used $\ln(\hat{\lambda} + 1)$. We repeated these analyses using both T_E and T_Q to test the scaling of the final decline to both total extinction and quasi-extinction, respectively. All model simulations and statistical analyses were performed using R v. 2.4.1.

3. RESULTS

(a) Extension of theoretical scaling rules

Results of our model simulations did not change qualitatively across the range of environmental stochasticity examined. For brevity, we therefore report only model results at intermediate levels of environmental stochasticity ($\beta = 2$), but the patterns reported apply equally to the range of tested values for β (0.5–5). Simulated populations started at carrying capacity, and most fluctuated around

carrying capacity for some time (depending largely on the magnitude of K), and then rapidly declined to extinction.

Our model simulations demonstrate that the scaling rules, predicted by Lande *et al.* (2003) for the special case where density dependence moderates only population growth after the carrying capacity has been reached (when $\theta \rightarrow \infty$), may in part be generalized to a broader range of types of density-dependent population growth. Specifically, our simulations show that hypothesis 1.1, which $T_K \gg T_E$, applies for all types of density-dependent growth examined ($p \ll 0.0001$ for all combinations of θ , K and $\ln(\lambda)$). The difference between $\ln(T_K)$ and $\ln(T_E)$ for model-simulated populations increased logarithmically with K , regardless of the value of θ . Absolute differences between T_K and T_E ranged from 2 or 3 time steps at low K to more than 25 000 time steps at the highest values of K examined.

Our simulations demonstrate that hypotheses 1.2 and 1.3, however, have a much more limited application. At high values of θ , although at values below infinity used in the ceiling model, scaling rules of hypotheses 1.2 [$T_E \propto \ln(K)$] and 1.3 [$T_E \propto 1/\ln(\lambda)$] still apply (as

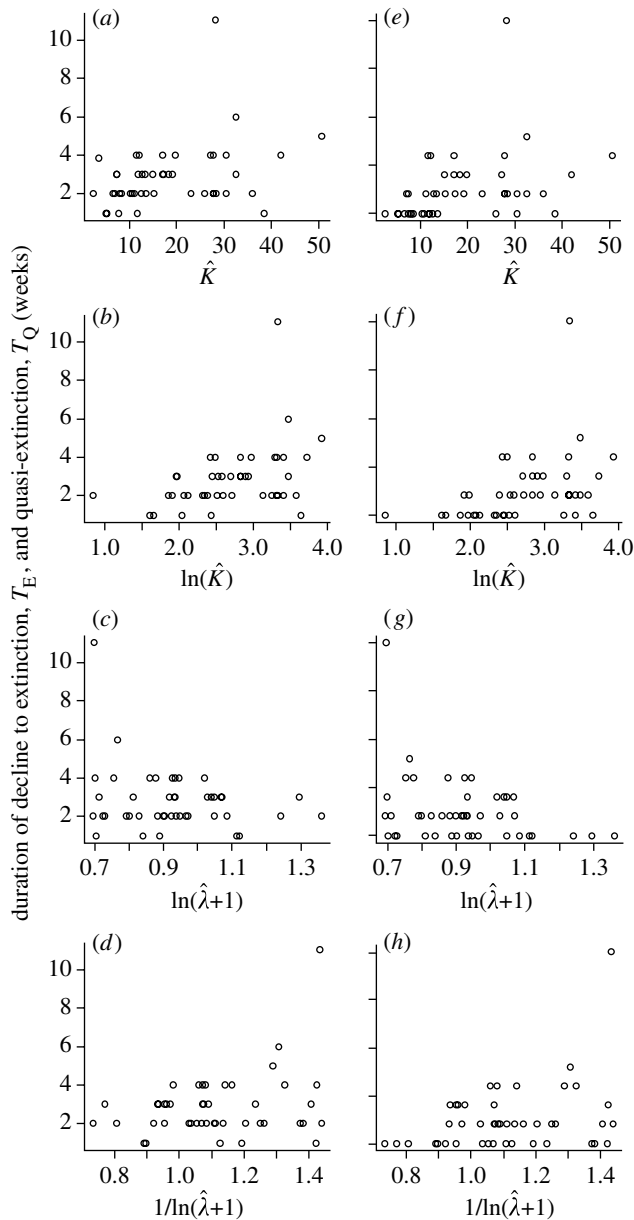


Figure 3. Duration of final decline to extinction as a function of (a, e) carrying capacity, K ; (b, f) $\ln(K)$; (c, g) intrinsic rate of increase, $\ln(\lambda + 1)$; and (d, h) $1/\ln(\lambda + 1)$. (a–d) Time to total extinction, T_E and (e–h) time to quasi-extinction, T_Q .

indicated by the best fit of linear model 4 to the simulated data; figure 2). However, at lower values of θ the scaling rules are much less clear, as alternative models were selected (figure 2). To examine this more closely, we varied θ more finely within this transition range and found that the cut-off is around $\theta = 2.49$. Above this cut-off, scaling rules proposed by Lande *et al.* (2003) apply; below this cut-off, scaling of the final decline to extinction is less clear, with model selection most frequently showing the best fit to simulated data by linear models 1 or 2 (appendix II). All coefficients in linear models 1–4 were highly significant ($p \ll 0.0001$) for all model simulations, except for simulations at $\theta = 0.1$, where none of the coefficients that including λ were significant.

(b) Empirical tests of scaling rules

Most of the 45 populations rose quickly from the initial population size of five individuals to carrying capacity, fluctuated around carrying capacity for some time and

then rapidly declined to extinction (see plots of time series from all 96 experimental populations in appendix III). Support for hypotheses 1.1–1.3 was similar when examining both the decline to final extinction and the decline to quasi-extinction.

parameters	total extinction, T_E			quasi-extinction, T_Q		
	p -value	AIC	Δ AIC	p -value	AIC	Δ AIC
<i>model 1</i>						
$\ln(\lambda + 1)$	0.31	172.89	1.26	0.15	175.02	1.55
K	0.05			0.07		
<i>model 2</i>						
$1/\ln(\lambda + 1)$	0.21	172.33	0.70	0.12	174.61	1.13
K	0.05			0.07		
<i>model 3</i>						
$\ln(\lambda + 1)$	0.31	172.20	0.56	0.16	173.89	0.41
$\ln(K)$	0.03			0.04		
<i>model 4</i>						
$1/\ln(\lambda + 1)$	0.21	171.63	0	0.12	173.47	0
$\ln(K)$	0.04			0.04		

then rapidly declined to extinction (see plots of time series from all 96 experimental populations in appendix III). Support for hypotheses 1.1–1.3 was similar when examining both the decline to final extinction and the decline to quasi-extinction.

Hypothesis 1.1 (T_E or $T_Q \ll T_K$): Consistent with the theoretical predictions, time before the final decline to extinction (15.8 ± 11.0 weeks, mean \pm s.d.) was longer than the duration of the final approach to extinction (2.8 ± 1.7 weeks) (Wilcoxon signed-rank test, $p \ll 0.0001$; figure 3). The results were qualitatively unchanged when comparing the time before the final decline to the duration of the decline to quasi-extinction (2.2 ± 1.7 weeks, $p \ll 0.0001$).

Hypotheses 1.2 and 1.3 (T_E or T_Q increases proportionally with $\ln(K)$ and with $1/\ln(\lambda + 0.1)$): Experimental results provided mixed support for these predicted scaling rules. Specifically, when examining the decline to final extinction (T_E), none of the terms with $\hat{\lambda}$ in models 1–4 were significant, while all the terms with \hat{K} were significant (table 1, figure 4). This supports the hypothesis that T_E scales proportionally with $\ln(K)$ (hypothesis 1.2), but does not support the hypothesis that T_E scales with $1/\ln(\lambda + 0.1)$ (hypothesis 1.3). However, model selection of the linear models with experimental data did not detect a difference between any of the models, indicating that T_E scaled just as closely with untransformed \hat{K} as with $\ln(\hat{K})$, (table 1, figure 3a–d). These patterns were replicated closely when examining the decline to quasi-extinction, with the exception that terms with untransformed \hat{K} were also marginally non-significant, while terms with $\ln(\hat{K})$ were significant (table 1), lending additional support to hypothesis 1.2 (figure 3e–h).

4. DISCUSSION

In this paper, we report that the scaling rules for the final decline to population extinction given by Lande *et al.* (2003) partially extend to a broader range of density-dependent

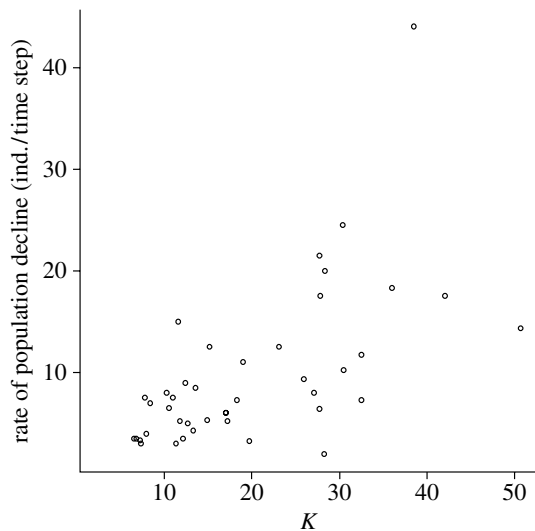


Figure 4. Proportional decline in population size during each time step of the final decline to extinction as a function of carrying capacity, K . $\text{Ind./time step} = 0.44 \times K + 1.08$, $F_{1,43} = 24.28$, $p < 0.001$.

conditions. Hypothesis 1.1 (T_E or $T_Q \ll T_K$) applied across the entire range of conditions examined. By contrast, hypotheses 1.2 and 1.3 (T_E or T_Q increases proportionally with $\ln(K)$ and with $1/\ln(\lambda + 0.1)$) were applicable only when density dependence is relatively unimportant for populations that are below K , i.e. under the ceiling model conditions used by Lande *et al.* (2003). When density dependence also influences populations that are far below K ($\theta < 2.49$), other scaling relationships apply (figure 2). We also note here that demographic stochasticity is an important driver of extinction dynamics and that this may more appropriately be modelled using a discrete process. However, we used a diffusion model for consistency with the original scaling rules proposed by Lande *et al.* (2003) so that deviations from their predictions under different density-dependent conditions could not be attributed to differences in modelling approaches. Our experimental results provide mixed support for the scaling rule predictions. Specifically, we found strong support for the prediction that the duration of final decline is small relative to population persistence prior to extinction (hypothesis 1.1). Our data also supported the more specific prediction that the duration of the final decline to extinction scales with $\ln(K)$ (hypothesis 1.2). However, our data did not support the prediction that the duration of the final decline to extinction scales with the inverse of the long-run population growth rate (hypothesis 1.3).

Laboratory experiments provide a valuable venue for testing population extinction theory (Griffen & Drake 2008b). Our laboratory system allowed strict control of factors affecting carrying capacity and population growth rate, but may have provided a stringent test of the scaling rules for the final decline to extinction. Experimental variations in $\hat{\lambda}$ and \hat{K} resulting from our experiments were relatively small compared with variations that might be expected under natural conditions where habitat size and quality can themselves be much more variable, and are combined with variation in other environmental variables such as temperature, availability of refuge habitat and the densities of interacting species. In addition, the food resource we used (*Spirulina*) is less nutritious than live

algae and subsequently supports fairly small clutch sizes at food levels used in our experiment (1.9 ± 0.9 mean \pm s.d., B. D. Griffen, unpublished data). This probably resulted in a lower range of population growth rates than are to be expected under natural conditions. Our laboratory experiments therefore provided less resolution (i.e. a smaller range of values) for $\hat{\lambda}$ and \hat{K} than that may be expected in the field, reducing our power to discriminate subtle differences in the relationships between these population parameters and the duration of the final decline to extinction. These limitations of the experimental system are modest and unlikely to lead to spurious conclusions.

We found that the duration of the final decline to extinction increased with the logarithm of carrying capacity and with untransformed carrying capacity (hypothesis 1.2, figure 3a,b). T_E may increase with K either because the rate of population decline is constant, but the population has farther to fall when K is higher, or because the rate of population decline decreases as K increases. To differentiate between these two scenarios, we examined the rate of decline for each population during the final decline to extinction as a function of K . Neither of these two scenarios occurred in our experiment; rather, the decline rate was higher for populations with larger K (figure 4), suggesting that while populations with larger K fell to extinction at a faster rate, this was more than that compensated by the greater distance they had to fall, and a net effect of longer duration of the final decline to extinction with larger K . A previous analysis of these data demonstrated overall time to population extinction increased with K (Griffen & Drake 2008a). Confirmation of hypothesis 1.1 demonstrates that at least a part of this effect is accounted for by the increased time before a population enters the final decline. Results here, however, show that increasing K has the further beneficial effect of lengthening the extinction process once the final decline has begun (figure 3a,b).

Our experimental data did not support the model-predicted relationship between T_E and population growth rate (hypothesis 1.3). The reason for this discrepancy is unclear and warrants further investigation.

The success of scaling rules across a broad range of ecological relationships provides a promising step towards ecological prediction. Predicting population extinction is a major goal of ecology (Clark *et al.* 2001), for instance in population viability analyses of threatened and endangered species (Morris & Doak 2002). However, much of the extinction process, particularly the final decline, is influenced by stochastic processes that hamper prediction. Reliable scaling rules for extinction, which incorporate this stochasticity, would therefore be broadly applicable and desirable. Our examination of the scaling rules, suggested by Lande *et al.* (2003) at a broad range of density-dependent conditions, broadens the applicability of hypothesis 1.1 to a wide range of natural systems that experience different forms of density dependence (Sibly *et al.* 2005), but suggests that hypotheses 1.2 and 1.3 may apply to a more limited set of populations. The lack of empirical support from our experiment for one of these scaling rules [$T_E \propto 1/\ln(\lambda)$] suggests that important aspects of the extinction process remain to be explained. However, empirical support for the other scaling rules suggests that they accurately capture the dynamics of the extinction processes, including the duration of the final decline.

We thank anonymous reviewers for their comments that greatly improved the manuscript. This research was supported by the University of Georgia, Odum School of Ecology and a grant from the University of Georgia Research Foundation and by the University of South Carolina.

REFERENCES

- Belgrano, A., Allen, A. P., Enquist, B. J. & Gillooly, J. F. 2002 Allometric scaling of maximum population density: a common rule for marine phytoplankton and terrestrial plants. *Ecol. Lett.* **5**, 611–613. (doi:10.1046/j.1461-0248.2002.00364.x)
- Bellwood, D. R. & Hughes, T. P. 2001 Regional-scale assembly rules and biodiversity of coral reefs. *Science* **292**, 1532–1534. (doi:10.1126/science.1058635)
- Belovsky, G. E., Mellison, C., Larson, C. & Van Zandt, P. A. 1999 Experimental studies of extinction dynamics. *Science* **286**, 1175–1177. (doi:10.1126/science.286.5442.1175)
- Carbone, C. & Gittleman, J. L. 2002 A common rule for the scaling of carnivore density. *Science* **295**, 2273–2276. (doi:10.1126/science.1067994)
- Clark, J. S. *et al.* 2001 Ecological forecasts: an emerging imperative. *Science* **293**, 657–660. (doi:10.1126/science.293.5530.657)
- Damuth, J. D. 1998 Common rules for animals and plants. *Nature* **395**, 115–116. (doi:10.1038/25843)
- Desharnais, R. A., Costantino, R. F., Cushing, J. M., Henson, S. M., Dennis, B. & King, A. A. 2006 Experimental support of the scaling rule for demographic stochasticity. *Ecol. Lett.* **9**, 537–547. (doi:10.1111/j.1461-0248.2006.00903.x)
- Diamond, J. M. 1984 'Normal' extinction of isolated populations. In *Extinctions* (ed. M. H. Nitecki), pp. 191–246. Chicago, IL: University of Chicago Press.
- Enquist, B. J., West, G. B., Charnov, E. L. & Brown, J. H. 1999 Allometric scaling of production and life-history variation in vascular plants. *Nature* **401**, 907–911. (doi:10.1038/44819)
- Fagan, W. F. & Holmes, E. E. 2006 Quantifying the extinction vortex. *Ecol. Lett.* **9**, 51–60. (doi:10.1111/j.1461-0248.2005.00845.x)
- Griffen, B. D. & Drake, J. M. 2008a Effects of habitat quality and size on extinction in experimental populations. *Proc. R. Soc. B.* **275**, 2251–2256. (doi:10.1098/rspb.2008.0518)
- Griffen, B. D. & Drake, J. M. 2008b Extinction in experimental populations. *J. Anim. Ecol.* **77**, 1274–1287. (doi:10.1111/j.1365-2656.2008.01426.x)
- Jetz, W., Carbone, C., Fulford, J. & Brown, J. H. 2004 The scaling of animal space use. *Science* **306**, 266–268. (doi:10.1126/science.1102138)
- Johnson, N. L., Kotz, S. & Kemp, W. 1993 *Univariate discrete distributions*, 2nd edn. New York, NY: Wiley.
- Lande, R. 1993 Risks of population extinction from demographic and environmental stochasticity and random catastrophes. *Am. Nat.* **142**, 911–927. (doi:10.1086/285580)
- Lande, R., Engen, S. & Sæther, B. E. 2003 *Stochastic population dynamics in ecology and conservation*. New York, NY: Oxford University Press.
- Lande, L., Engen, S., Sæther, B. E. & Coulson, T. 2006 Estimating density dependence from time series of population age structure. *Am. Nat.* **168**, 76–87. (doi:10.1086/504851)
- Meir, E. & Fagan, W. F. 2000 Will observation error and biases ruin the use of simple extinction models? *Conserv. Biol.* **14**, 148–154. (doi:10.1046/j.1523-1739.2000.98502.x)
- Middleton, D. A., Veitch, A. R. & Nisbet, R. M. 1995 The effects of an upper limit to population size on persistence time. *Theor. Popul. Biol.* **48**, 277–305. (doi:10.1006/tpbi.1995.1030)
- Morris, W. F. & Doak, D. F. 2002 *Quantitative conservation biology: theory and practice of population viability analysis*. Sunderland, MA: Sinauer Associates.
- Otto, S. B., Rall, B. C. & Brose, U. 2007 Allometric degree distributions facilitate food-web stability. *Nature* **450**, 1226–1229. (doi:10.1038/nature06359)
- Savage, V. M., Gillooly, J. F., Brown, J. H., West, G. B. & Charnov, E. L. 2004 Effects of body size and temperature on population growth. *Am. Nat.* **163**, 429–441. (doi:10.1086/381872)
- Schneider, D. C. 2001 The rise of the concept of scale in ecology. *Bioscience* **51**, 545–553. (doi:10.1641/0006-3568(2001)051[0545:TROTCO]2.0.CO;2)
- Sibly, R. M., Barker, D., Denham, M. C., Hone, J. & Pagel, M. 2005 On the regulation of populations of mammals, fish, and insects. *Science* **309**, 607–610. (doi:10.1126/science.1110760)
- Sims, D. W. *et al.* 2008 Scaling laws of marine predator search behaviour. *Nature* **451**, 1098–1102. (doi:10.1038/nature06518)
- Turchin, P. 2003 *Complex population dynamics: a theoretical/empirical synthesis*. Princeton, NJ: Princeton University Press.
- USEPA 2002 *Methods for measuring the acute toxicity of effluents and receiving waters to freshwater and marine organisms*, 5th edn. Washington, DC: Office of Water, U.S. Environmental Protection Agency. EPA-821-R-02-012.
- Volkov, I., Banavar, J. R., Hubbell, S. P. & Maritan, A. 2007 Patterns of relative species abundance in rainforests and coral reefs. *Nature* **450**, 45–49. (doi:10.1038/nature06197)